

## De Novo Design of Protein Function: Predictable Structure–Function Relationships in Synthetic Redox Proteins

Mitchell W. Mutz,<sup>†</sup> Martin A. Case,<sup>†,‡</sup> James F. Wishart,<sup>§</sup>  
M. Reza Ghadiri,<sup>‡</sup> and George L. McLendon<sup>\*,†</sup>

Department of Chemistry, Princeton University  
Princeton, New Jersey 08544

Departments of Chemistry and Molecular Biology, and  
the Skaggs Institute of Chemical Biology  
The Scripps Research Institute  
10555 North Torrey Pines Road  
La Jolla, California 92037

Chemistry Department, Brookhaven National Laboratory  
Upton, New York 11973

Received August 10, 1998

Recent advances in theoretical and experimental protein design have begun to demonstrate an ability to construct specific structural motifs from first principles. However, the design and experimental confirmation of function in de novo proteins remains rare. Redox (electron transfer) function is quite common in proteins and offers a well-defined target for the demonstration of designed structure–function relationships. The factors which determine electron-transfer rates and pathways in natural proteins are well-understood, allowing a validation of synthetic systems.<sup>1–4</sup> Moreover, designed proteins offer robust structures, which are likely to be better models of biological electron transfer than small peptide systems. Indeed, structural studies of small helical peptides in solution yield evidence of transiently stable secondary structure.<sup>5</sup>

There have been numerous reports of de novo designed synthetic helix bundle motifs<sup>6–11</sup> which may incorporate redox-active sites.<sup>12–15</sup> The candidate of choice for these studies is a parallel three-helix bundle architecture incorporating a redox-active N-terminal ruthenium(II)tris-bipyridyl moiety.<sup>6</sup> Ru<sup>II</sup>(bpy)<sub>3</sub>. This construct offers a well-characterized structure which lends itself readily to electron-transfer studies not only by virtue of its

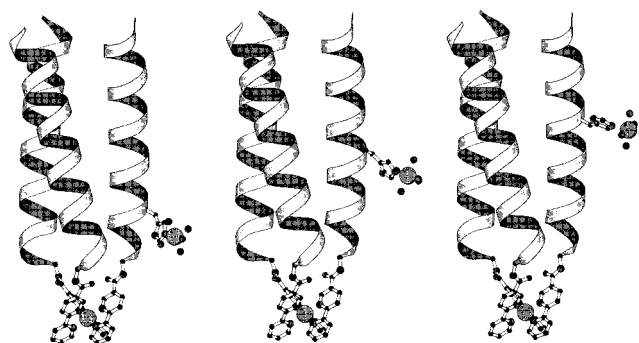


**Figure 1.** Models of Ru<sup>II</sup>( $\alpha p$ )<sub>2</sub>( $\alpha p$ 5)–Ru<sup>III</sup>(NH<sub>3</sub>)<sub>5</sub>, Ru<sup>II</sup>( $\alpha p$ )<sub>2</sub>( $\alpha p$ 9)–Ru<sup>III</sup>(NH<sub>3</sub>)<sub>5</sub>, and Ru<sup>II</sup>( $\alpha p$ )<sub>2</sub>( $\alpha p$ 12)–Ru<sup>III</sup>(NH<sub>3</sub>)<sub>5</sub> bundles (left to right). The N-terminal bipyridine moieties are shown at the bottom of the figure.<sup>18</sup>

structural integrity but also due to the photophysical properties of the Ru<sup>II</sup>(bpy)<sub>3</sub> group.<sup>16</sup>

Four 20-residue peptides based on the  $\alpha p$  consensus sequence were synthesized

	1	5	10	15	20
$\alpha p$ :	bpy-gly-glu-leu-ala-gln-lys-leu-glu-gln-ala-leu-gln-lys-leu-glu-gln-ala-leu-gln-lys-amide				
$\alpha p$ 5:	bpy-gly-glu-leu-ala-gln-lys-leu-glu-gln-ala-leu-gln-lys-leu-glu-gln-ala-leu-gln-lys-amide	his			
$\alpha p$ 9:	bpy-gly-glu-leu-ala-gln-lys-leu-glu-gln-lys-leu-glu-gln-ala-leu-gln-lys-amide		his		
$\alpha p$ 12:	bpy-gly-glu-leu-ala-gln-lys-leu-glu-gln-lys-leu-glu-gln-ala-leu-gln-lys-amide			his	

where bpy is 5-carboxy-2,2'-bipyridine.

These peptides, which are predisposed to form amphiphilic helical structures, have previously been shown to self-assemble into topologically predetermined parallel three-helix bundle metalloproteins upon stereoselective complexation of the N-terminal bpy ligands to Ru<sup>II</sup> ions.<sup>6,12</sup>

To probe the electron-transfer properties of Ru<sup>II</sup>( $\alpha p$ )<sub>3</sub>, histidine residues were introduced into the  $\alpha p$  sequences at solvent-exposed positions 5, 9, or 12 to provide attachment sites for redox-active Ru<sup>III</sup>(NH<sub>3</sub>)<sub>5</sub> moieties<sup>17</sup> as shown in Figure 1. These derivatives of the  $\alpha p$  parent peptide were designated  $\alpha p$ 5,  $\alpha p$ 9, and  $\alpha p$ 12. The heterotrimeric three-helix bundles investigated were thus Ru<sup>II</sup>( $\alpha p$ )<sub>2</sub>( $\alpha p$ 5), Ru<sup>II</sup>( $\alpha p$ )<sub>2</sub>( $\alpha p$ 9), and Ru<sup>II</sup>( $\alpha p$ )<sub>2</sub>( $\alpha p$ 12). The direct distances between the electron-acceptor groups of these molecules can be predicted from the well-established  $\alpha$ -helical pitch of 1.5 Å vertical translation per residue. Hence, there should be about a 6 Å vertical displacement between the Ru<sup>III</sup>(NH<sub>3</sub>)<sub>5</sub> groups on the Ru<sup>II</sup>( $\alpha p$ )<sub>2</sub>( $\alpha p$ 5) and Ru<sup>II</sup>( $\alpha p$ )<sub>2</sub>( $\alpha p$ 9) proteins, and a 4.5 Å vertical displacement between the Ru<sup>III</sup>(NH<sub>3</sub>)<sub>5</sub> groups on the Ru<sup>II</sup>( $\alpha p$ )<sub>2</sub>( $\alpha p$ 9) and Ru<sup>II</sup>( $\alpha p$ )<sub>2</sub>( $\alpha p$ 12) proteins. The actual change in donor–acceptor distances is 6.3 Å and 4.2 Å, respectively, as determined by molecular modeling.<sup>18</sup> The incorporation of the Ru<sup>III</sup>(NH<sub>3</sub>)<sub>5</sub> modifier produces no observable change of the helical content of the bundles; such structural integrity upon modification with redox-active groups is an essential requirement for a systematic study of the distance dependence of intramolecular electron transfer.

Since molecular electron-transfer rates scale exponentially with distance,<sup>19</sup> a 6 Å displacement is predicted to change the electron-transfer rate by nearly 3 orders of magnitude. We used two

\* Correspondence author. E-mail: glm@chemvax.princeton.edu.

<sup>†</sup> Princeton University.

<sup>‡</sup> The Scripps Research Institute.

<sup>§</sup> Brookhaven National Laboratory.

(1) Beratan, D. N.; Betts, J. N.; Onuchic, J. N. *Science* **1991**, 252, 1285–1288.

(2) Beratan, D. N.; Onuchic, J. N.; Winkler, J. R.; Gray, H. B. *Ann. Rev. Biophys. Biomol. Struct.* **1992**, 21, 349–377.

(3) Evenson, J. W.; Karplus, M. *Science* **1993**, 262, 1247–1249.

(4) Moser, C. C.; Keske, J. M.; Warncke, K.; Farid, R. S.; Dutton, P. L. *Nature* **1992**, 335, 796–802.

(5) Wright, P. E.; Dyson, H. J.; Lerner, R. A. *Biochemistry* **1988**, 27, 7167–7175.

(6) Ghadiri, M. R.; Soares, C.; Choi, C. *J. Am. Chem. Soc.* **1992**, 114, 825–831.

(7) Bryson, J. W.; Betz, S. F.; Lu, H. S.; Suich, D. J.; Zhou, H. X. X.; O'Neil, K. T.; DeGrado, W. F. *Science* **1995**, 270, 935–941.

(8) Handel, T.; DeGrado, W. F. *J. Am. Chem. Soc.* **1990**, 112, 6710–6711.

(9) Lieberman, M.; Sasaki, T. *J. Am. Chem. Soc.* **1991**, 113, 1470–1471.

(10) Hill, C. P.; Anderson, D. H.; Wesson, L.; DeGrado, W. F.; Eisenberg, D. *Science* **1990**, 249, 543–546.

(11) Hecht, M. H.; Richardson, J. S.; Richardson, D. C.; Ogden, R. C. *Science* **1990**, 249, 884–891.

(12) (a) Ghadiri, M. R.; Case, M. A. *Angew. Chem., Int. Ed. Engl.* **1993**, 32, 1594–1597. (b) Case, M. A.; Ghadiri, M. R.; Mutz, M. W.; McLendon, G. L. *Chirality* **1998**, 10, 35–40. (c) For this work it was necessary to develop a “mixed bundle” synthetic strategy, in which only one helix is labeled with the histidine–ruthenium acceptor. Zhou, J.; Case, M. A.; Wishart, J. F.; McLendon, G. L. *J. Phys. Chem.* **1998**, 102, 9975–9980.

(13) Choma, C. T.; Lear, J. D.; Nelson, M. J.; Dutton, P. L.; Robertson, D. E.; DeGrado, W. F. *J. Am. Chem. Soc.* **1994**, 116, 856–865.

(14) Mutz, M. W.; McLendon, G. L.; Wishart, J. F.; Gaillard, E. R.; Corin, A. F. *Proc. Natl. Acad. Sci. U.S.A.* **1996**, 93, 9521–9526.

(15) Rabanal, F.; Gibney, B. R.; DeGrado, W. F.; Moser, C. C.; Dutton, P. L. *Inorg. Chim. Acta* **1996**, 243, 213–218.

(16) Sutin, N.; Creutz, C. *Pure Appl. Chem.* **1980**, 52, 2717–2738.

(17) Yocum, K. M. et al. *Proc. Natl. Acad. Sci. U.S.A.* **1982**, 79, 7052–7055.

(18) The minimum energy conformations of the Ru<sup>III</sup>(NH<sub>3</sub>)<sub>5</sub>(His) side chains were calculated with Discover 3 (Molecular Simulations Incorporated) using the *esff* forcefield.

(19) Marcus, R. A.; Sutin, N. *Biochim. Biophys. Acta* **1985**, 811, 265–322.

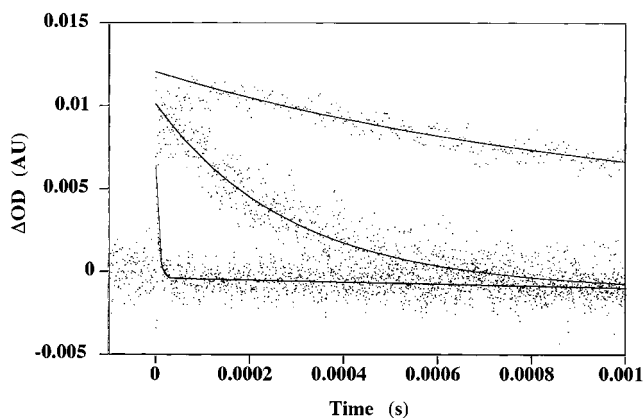
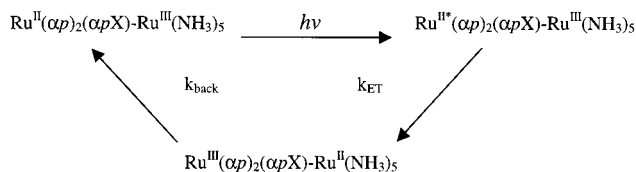


**Figure 2.** Pulse radiolysis transient absorption signals for  $\text{Ru}^{\text{II}}(\alpha p)_2(\alpha p12)-\text{Ru}^{\text{III}}(\text{NH}_3)_5$  (upper),  $\text{Ru}^{\text{II}}(\alpha p)_2(\alpha p9)-\text{Ru}^{\text{III}}(\text{NH}_3)_5$  (center), and  $\text{Ru}^{\text{II}}(\alpha p)_2(\alpha p5)-\text{Ru}^{\text{III}}(\text{NH}_3)_5$  (lower) monitored at 380 nm to observe the decay of the  $\text{Ru}^{\text{I}}(\alpha p)_2(\alpha pX)$  species. Note that the decay of  $\text{Ru}^{\text{I}}(\alpha p)_2(\alpha p5)-\text{Ru}^{\text{III}}(\text{NH}_3)_5$  is ten times faster than indicated by the abscissa scale. Experimental conditions are given in Supporting Information.

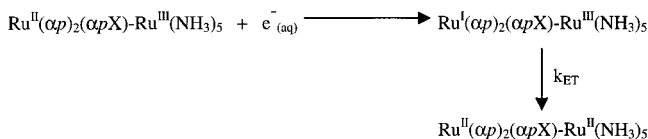
complementary techniques, flash photolysis and pulse radiolysis, to provide appropriate time windows to characterize the electron-transfer kinetics of these systems. Flash photolysis was performed on both  $\text{Ru}^{\text{II}}(\alpha p)_2(\alpha p5)$  and  $\text{Ru}^{\text{II}}(\alpha p)_2(\alpha p9)$  modified with  $\text{Ru}^{\text{III}}(\text{NH}_3)_5$  according to the following:



$X = 5$  or  $9$ , and  $\text{Ru}^{\text{II}*}$  is the excited state of the  $\text{Ru}^{\text{II}}(\text{bpy})_3$  moiety.

The unmodified metalloproteins  $\text{Ru}^{\text{II}}(\alpha p)_2(\alpha p5)$  and  $\text{Ru}^{\text{II}}(\alpha p)_2(\alpha p9)$  were both found to have excited-state lifetimes of 116 ns; however, for  $\text{Ru}^{\text{II}}(\alpha p)_2(\alpha p5)-\text{Ru}^{\text{III}}(\text{NH}_3)_5$  the excited-state lifetime was 79 ns. The difference in excited-state lifetimes corresponds to an electron-transfer rate constant of  $4.0 \times 10^6 \text{ s}^{-1}$  (see Supporting Information). In contrast, no change in excited-state lifetime was observed for  $\text{Ru}^{\text{II}}(\alpha p)_2(\alpha p9)-\text{Ru}^{\text{III}}(\text{NH}_3)_5$  since  $k_{\text{ET}}$  is substantially less than the  $\text{Ru}^{\text{II}*}(\alpha p)_2(\alpha p9)$  intrinsic excited-state decay rate of  $8.6 \times 10^6 \text{ s}^{-1}$ . Given this trend, the system  $\text{Ru}^{\text{II}}(\alpha p)_2(\alpha p12)-\text{Ru}^{\text{III}}(\text{NH}_3)_5$  was not investigated by flash photolysis.

Pulse radiolysis was also used to measure electron transfer rates in the  $\text{Ru}^{\text{II}}(\alpha p)_2(\alpha pX)-\text{Ru}^{\text{III}}(\text{NH}_3)_5$  systems according to



$X = 5, 9$ , or  $12$ , and  $\text{Ru}^{\text{I}}$  represents the ruthenium tris-bipyridine radical anion complex.

For  $\text{Ru}^{\text{II}}(\alpha p)_2(\alpha p5)-\text{Ru}^{\text{III}}(\text{NH}_3)_5$ , the rate constant  $k_{\text{ET}} = 3 \times 10^6 \text{ s}^{-1}$  was calculated from the time and amplitude resolved radiolysis data (Figure 2). This is close to the limit of resolution of this method as adopted in this work. Conversion of the kinetic to thermodynamic product was easily measured for  $\text{Ru}^{\text{II}}(\alpha p)_2(\alpha p9)-\text{Ru}^{\text{III}}(\text{NH}_3)_5$  which exhibited  $k_{\text{ET}} = 2.9 \times 10^3 \text{ s}^{-1}$  (Figure 2). This rate constant is clearly consistent with the limit of  $k_{\text{ET}} < 8 \times 10^6 \text{ s}^{-1}$  set by the photolysis experiments at a lower driving force. In the case of  $\text{Ru}^{\text{II}}(\alpha p)_2(\alpha p12)-\text{Ru}^{\text{III}}(\text{NH}_3)_5$ , the rate of electron transfer was too slow to be measured within the lifetime

**Table 1.** Rate Constants and Driving Forces for  $\text{Ru}^{\text{II}}(\alpha p)_2(\alpha pX)-\text{Ru}^{\text{III}}(\text{NH}_3)_5$  Systems<sup>a</sup>

	radiolysis ( $\text{s}^{-1}$ )	photolysis ( $\text{s}^{-1}$ )
$\text{Ru}^{\text{II}}(\alpha p)_2(\alpha p5)-\text{Ru}^{\text{III}}(\text{NH}_3)_5$	$3.0 \times 10^6$	$4.0 \times 10^6$
$\text{Ru}^{\text{II}}(\alpha p)_2(\alpha p9)-\text{Ru}^{\text{III}}(\text{NH}_3)_5$	$2.9 \times 10^3$	<i>b</i>
$\text{Ru}^{\text{II}}(\alpha p)_2(\alpha p12)-\text{Ru}^{\text{III}}(\text{NH}_3)_5$	$< 1 \times 10^2$	<i>b</i>
$\Delta G^\circ_{\text{estimated}}$ (V)	-1.2	-1.0

<sup>a</sup> Experimental conditions are given in Supporting Information. <sup>b</sup> Too slow to measure.

of the  $\text{Ru}^{\text{I}}(\alpha p)_2(\alpha p12)$  species. This allows us to place an upper limit of  $100 \text{ s}^{-1}$  on the electron-transfer rate constant for this molecule.

With these electron-transfer rates in hand, one can estimate  $\beta$ , the distance-dependent electronic coupling in the  $\alpha p$  series according to  $\ln k \propto (-\beta R)$  where  $R$  is the donor-acceptor distance.

From the data in Table 1, we derive a value of  $\beta = 1.2 \pm 0.1 \text{ \AA}^{-1}$ . The value of  $\beta$  has been measured in a variety of protein systems and generally falls between 0.9 and  $1.4 \text{ \AA}^{-1}$  depending on the precise details of the structure and the associated electron transfer "pathways" between donor and acceptor.<sup>20,21</sup> The effective electronic coupling of the  $\text{Ru}^{\text{II}}(\alpha p)_3$  series is thus placed firmly within the range of  $\beta$  determined for natural proteins. It is noteworthy that previous studies of electron transfer within a single helix have revealed neither  $\beta$  values consistent with natural proteins nor evidence of helix-mediated electron transfer.<sup>24</sup> The present study also shows that the experimental value of  $\beta = 1.2 \pm 0.1 \text{ \AA}^{-1}$  falls within the range expected from theoretical pathway models of through-helix electron transfer.<sup>25</sup> We also note that comparison of the photolysis rates with the radiolysis rates allows a good estimate to be made for the reorganization energy,  $\lambda$ , in the relationship  $k_{\text{ET}} = k_{\text{max}} \exp[-(\Delta G^\circ + \lambda)^2/4\lambda k_{\text{B}}T]$  where  $\Delta G^\circ$  is reaction free energy,  $\lambda$  is reorganization energy,  $k_{\text{B}}$  is the Boltzmann constant, and  $T$  is temperature.<sup>19</sup> We infer that for this system  $\lambda = 1.1 \text{ V}$ , in line with expectations from related systems. Extrapolation to a van der Waals' contact distance of between 6.6 and 8.6  $\text{\AA}$  then predicts a reasonable maximum rate of between  $10^{10}$  and  $10^{11} \text{ \AA}^{-1}$ .

The de novo designed redox proteins described show measured electron-transfer rates fully consistent with current theory. These data show for the first time that it is possible to design functional proteins whose reactivity can be *predicted* from structure with quantitative precision. The observation of a strong distance dependence over several orders of magnitude in time confirms that the helical structure is robust over the time regimes studied. Such designed proteins can offer a way to address questions of protein design and function within a single, well-defined motif that are difficult to address with natural proteins.

**Acknowledgment.** This work was supported by NIH Grants GM-48495 (M.R.G.) and GM-50019 (G.L.M.). Work at Brookhaven National Laboratory was carried out under contract DE-AC02-76H00016 with the U.S. Department of Energy and supported by its Division of Chemical Sciences, Office of Basic Energy Research.

**Supporting Information Available:** Flash photolysis transient emission data for  $\text{Ru}^{\text{II}}(\alpha p)_2(\alpha p5)$  and  $\text{Ru}^{\text{II}}(\alpha p)_2(\alpha p5)-\text{Ru}^{\text{III}}(\text{NH}_3)_5$  at 650 nm and experimental conditions for flash photolysis and pulse radiolysis experiments. This material is available free of charge via the Internet at <http://pubs.acs.org>.

JA9828612

(20) Axup, A. W.; Albin, M.; Mayo, S. L.; Crutchley, R. J.; Gray, H. B. *J. Am. Chem. Soc.* **1988**, *110*, 435-439.

(21) Casimiro, D. R.; Wong, L. L.; Colon, J. L.; Zewert, T. E.; Richards, J. H.; Chang, I. J.; Winkler, J. R.; Gray, H. B. *J. Am. Chem. Soc.* **1993**, *115*, 1485-1489.

(22) Liu, Y. P.; Newton, M. D. *J. Phys. Chem.* **1995**, *99*, 12382-12386.

(23) Brown, G.; Sutin, N. *J. Am. Chem. Soc.* **1979**, *101*, 883-892.

(24) Inai, Y.; Sisido, M.; Imanishi, Y. *J. Phys. Chem.* **1991**, *95*, 3847-3851.

(25) Langen, R.; Chang, I. J.; Germanas, J. P.; Richards, J. H.; Winkler, J. R.; Gray, H. B. *Science* **1995**, *268*, 1733-1735.